Associative plasticity of granule cell inputs to cerebellar Purkinje cells.

Rossella Conti and Céline Auger*

Université Paris Cité, CNRS, Saints-Pères Paris Institute for the Neurosciences

F-75006 PARIS FRANCE

* corresponding author

Abstract

Granule cells of the cerebellum make up to 175 000 excitatory synapses on a single Purkinje cell, encoding the wide variety of information from the mossy fibre inputs into the cerebellar cortex. The granule cell axon is made of an ascending portion and a long parallel fibre extending at right angles, an architecture suggesting that synapses formed by the two segments of the axon could encode different information. There are controversial indications that ascending axon (AA) and parallel fibre (PF) synapse properties and modalities of plasticity are different. We tested the hypothesis that AA and PF synapses encode different information, and that association of these distinct inputs to Purkinje cells might be relevant to the circuit and trigger plasticity, similarly to the coincident activation of PF and climbing fibre inputs. Here we describe a new form of associative plasticity between these granule cell inputs, and show for the first time that synchronous AA and PF repetitive train stimulation, with inhibition intact, triggers long term potentiation (LTP) at AA synapses specifically. Furthermore, the timing of presentation of the two inputs controls the outcome of plasticity and induction requires NMDAR and mGluR activation. These observations reinforce the suggestion that AA and PF synapses are two synaptic populations with different coding capabilities and plasticity. Associative plasticity of AA and PF synapses enables effective association of information transmitted via granule cells.

Introduction

The ability to discriminate self generated from external stimuli is essential to apprehend the world as movement itself activates sensory receptors. In fish, discrimination of self from external stimuli has been shown to rely on associating motor command and sensory feedback in cerebellar-like structures (Montgomery & Bodznick, 1994; Sawtell, 2017). This is achieved by modifying the motor inputs to generate a negative image of the associated sensory inputs, effectively subtracting the predictable sensory inputs. This way, only unpredicted inputs are output by the principal cells. While in most cases the role of the cerebellum in sensory information processing is still unclear, theoretical models and work on plasticity suggest that it might similarly be involved in cancellation of predictable sensory inputs, but distinct sensory and motor synapses have yet to be identified in the cerebellum. The role of the cerebellum in motor learning and coordination has been well documented, but it is now clear that it is also involved in a number of higher cognitive functions (Schmahmann & Sherman, 1998; Stoodley & Schmahmann, 2010). An intriguing possibility, in the wider context of the cerebellum, is that receptive field and contextual inputs are encoded differentially by the granule cell AA and PF synapses. These inputs might be functionally associated based on relative timing to subtract predictable inputs, and output only unpredicted inputs, as observed for motor and sensory inputs in cerebellar-like structures.

Sensorimotor information is delivered to the cerebellar cortex by mossy fibres and relayed by granule cells (GCs) to the Purkinje cells (PCs) and inhibitory network for integration. Anatomically, the axon of a GC first extends through the PC layer and into the molecular layer, making up the ascending portion of the axon (AA), then bifurcates at a right angle, forming two PFs that extend several millimetres along the folium. As a consequence, an AA can form multiple synapses with a few overlaying PCs in the same sagittal plane as the GC soma, distributing information to a restricted number of cells, whereas PFs course through the dendritic trees of hundreds of PCs along the lobule (Napper & Harvey, 1988), distributing information widely to other microzones. This morphology and functional data have suggested that PC activity might be principally driven by local GCs via AA synapses (Cohen & Yarom, 1998), while distant GCs might modulate its activity via the PF system to provide the PC with less specific contextual information.

In the adult rat, an estimated 175k excitatory PF synapses encode information on the dendritic tree of a single PC (Napper & Harvey, 1988). We previously identified two PF synaptic populations with different molecular signatures (Devi et al., 2016). However, PF synapses have usually been treated as a uniform

population, and we know little about the way the variety of information received by PCs is encoded at synaptic level. Isope and Barbour (Isope & Barbour, 2002) estimated that 85% of PF synapses are silent, as suggested by in vivo data (Ekerot & Jörntell, 2001), however that proportion was significantly lower for local GCs and presumably AA synapses. In this study and that by Walter (Walter et al., 2009), properties of AA synapses were found to be indistinguishable from PF synapses. On the other hand, a study by Sims and Hartell (2005), has shown that AA and PF synaptic properties and susceptibility to plasticity are different. AA synapses were shown to be refractory to plasticity with well described protocols. Neither associative CF-mediated long term depression (LTD) nor LTP could be induced (Sims & Hartell, 2005; Sims & Hartell, 2006). These observations, together with the anatomical properties of the GC axon, suggest that AA and PF synapses can transmit different types of information and play different roles in cerebellar computation.

In this study we asked whether coincident activation of AA and PF synapses might trigger specific synaptic plasticity of GC inputs, like associative activation with the CF. We show that a protocol pairing stimulation of AAs and PFs, with inhibition preserved, results in LTP of the AA inputs. AA-LTP is timing-dependent and relies on NMDAR and mGluR activation, bringing together these two pathways. $GABA_AR$ activation was also required for efficient induction and maintenance of plasticity. Finally we show that the different plasticity found for AA and PF inputs is not merely due to the differential spatial distribution of their synapses on the dendritic tree.

Methods

Ethical approval: Sprague Dawley rats were provided by Janvier (St Berthevin, France) or bred and subsequently housed at the Animal Housing and Breeding facility of BioMedTech facilities (INSERM US36, CNRS UAR2009, Université Paris Cité) in agreement with the European Directive 2010/63/UE regarding the protection of animals used for experimental and other scientific purposes. Experimental procedures were approved by the French Ministry of Research and the ethical committee for animal experimentation of Paris Cité.

Slice preparation: Experiments were performed on horizontal slices 300 µm thick cut from the cerebellum of 19-25 day-old Sprague-Dawley male or female rats. Briefly, rats were killed by decapitation under general anaesthesia following inhalation of the volatile anaesthetic isoflurane at a concentration of 3-4% in accordance with the Directive 2010/63/UE, and the cerebellum was quickly removed. After removal of the brainstem, the tissue was glued to the stage of a vibratome (Leica VT1200S, Germany).

Slices were cut at a temperature of 34° C and subsequently kept in a vessel bubbled with 95% O_2 / 5% CO_2 at this temperature. Slice preparation and recordings were made in a bicarbonate buffered solution containing in mM: 115 NaCl, 2.5 KCl, 1.3 NaH_2PO_4, 26 $NaHCO_3$, 2mM $CaCl_2$, 1mM $MgSO_4$, 0.1mM Ascorbic Acid, and 25 glucose.

Patch-clamp recording of synaptic currents: Whole-cell patch-clamp recordings were made from PCs, identified by their size and location at the edge of the molecular and GC layers, with an EPC10 amplifier (HEKA, Germany) and PatchMaster acquisition software. Bath temperature was kept at 30-32° C The internal solution contained in mM: 135 KGluconate, 10 K_2 Creatine Phosphate, 10 HEPES, 0.01 EGTA, 2.5 $MgCl_2$, 2 $ATPNa_2$ and 0.4 GTPNa, pH adjusted to 7.3 with KOH and osmolarity to 295 mOsm/kg. When filled with the internal solution, recording pipettes had a resistance between 3 and 4.0 MΩ. Membrane currents were recorded at a pipette potential of -60 mV (not corrected for junction potential of approximately -12 mV pipette-bath). Series resistance was 80-90 % compensated. During experiments, the preparation was visualised on an upright microscope (Olympus BFX51; 60x 0.9 NA water dipping objective) and the bath was continuously perfused at a rate of 5 ml/min (5 bath volumes per min) with solution equilibrated with 95% O_2 / 5% CO_2 to maintain pH and solution recirculated.

Plasticity of GC to PC synapses was studied in horizontal cerebellar slices as these slices better preserve PFs running in the plane of cut. At this age, GC synapses are well established (Ichikawa et al., 2016). AAs and PFs were stimulated with patch pipettes slightly larger than those used for recordings filled with a Hepes-buffered external solution and positioned either in the molecular (lower two thirds) or the GC layer, as discussed in the result section. The baseline amplitude of both AA and PF pathways were sampled with a pair of suprathreshold pulses at 50 ms interval, delivered every 10 s (Fig 1A top panel, stimulation was biphasic, 100-180 µs duration, 5 to 15V). The AA and PF test stimuli were separated by 0.5 s. In most of the experiments AAs were tested first to avoid possible interference from mGluRs activation and the release of endocannabinoid by PFs stimulation. No antagonist of the inhibitory inputs was applied. Evoked responses consisted of excitatory postsynaptic currents (EPSCs) that were often quickly followed by inhibitory postsynaptic currents (IPSCs) (mixed EPSC/IPSC, see supplementary material and supplementary fig.3). The low Cl^- concentration in the intracellular solution ensured the reversal potential for Cl^- was close to the value determined for PCs (-85 mV, (Chavas & Marty, 2003)), and IPSCs were outward at the recording potential of -60 mV. After recording a baseline period of at least 10 minutes, we applied a stimulation protocol aimed at inducing plasticity. The recording configuration was switched to Current clamp and the potential set near -65 mV. The protocol applied (see Fig. 1A bottom

panel) consisted in the synchronous stimulation of both inputs by a train of 15 pulses at 100 Hz repeated every 3 s a total of 100 times. Following the induction protocol, the recording configuration was returned to Voltage clamp and test of alternate AA- and PF-EPSC amplitude resumed. In the result section the number of cells sometimes differ for the two pathways for a given set of experiments, because one of the inputs was sometimes lost during the 30 minutes following induction. Because the protocol was properly applied, the data for the remaining input were included in the results.

Analysis of evoked EPSCs: For the analysis of synaptic currents, raw current traces were exported to Igor Pro (Wavemetrics) and peak excitatory current amplitudes were measured as the minimum of the synaptic response (mixed EPSC/IPSC) over a time window overlapping the peak and spanning a few sampling points of the average EPSC. Since the plasticity protocol might affect EPSCs and IPSCs differently, and might therefore affect our estimate of the peak EPSC and its long term changes, we conducted a set of experiments to measure the IPSCs and EPSCs separately and confirmed that measuring the minimum of the mixed EPSC/IPSC gives a good estimate of EPSC amplitude and its long term changes (see supplementary materials and supplementary figure 3).

Chemicals: 2-(3-Carboxypropyl)-3-amino-6-(4methoxyphenyl)pyridazinium bromide (SR 95531), D-(-)-2-Amino-5-phosphonopentanoic acid (D-AP5) and 7-(Hydroxyimino)cyclopropa[b]chromen-1a-carboxylate ethyl ester (CPCCOEt) were purchased from Tocris Bioscience or from HelloBio (UK). CPCCOEt was dissolved in DMSO at a concentration of 100mM. All other stocks were prepared in water. Drugs were diluted in saline just before use. All other chemicals were purchased from Sigma.

Statistical significance was tested with non-parametric methods for most of the data sets. These do not require assumptions about the nature of the distribution of the variables (as parametric tests do);we used either the Wilcoxon signed rank test (non-parametric, for paired samples) or the Wilcoxon Mann Whitney test (non-parametric, for unpaired samples). The T-test was used for control data only, where N was big enough to show a normal distribution of the variables (see Supplementary figure 1). Tests were conducted using Igor Pro (Wavemetrics). All values given are mean ± SEM.

Results

Associative plasticity of AA synapses. To test for associative plasticity between ascending axon and

parallel fibre inputs we positioned two separate stimulating electrodes to achieve activation of different GC inputs onto a recorded PC (Fig. 1A top panel). To stimulate PFs, a stimulation pipette was positioned in the molecular layer, 100 to 200 µm away from the dendritic tree of the recorded cell. The average length of a PF is between 4.2 and 4.7 mm (Pichitpornchai et al., 1994), therefore the vast majority of fibres stimulated in the molecular layer belong to GCs distant from the recorded cell. The probability that the stimulated fibres belong to GCs with somas lying close to the PC soma making AA synapses with the PC is of 1-2%. To stimulate AAs, a second stimulation pipette was positioned in the GC layer, within a narrow window centered on the PC somato-dendritic plane. The GCs stimulated in this position have a high probability of making AA synapses onto the dendritic tree of the PC, although a small proportion could also make synapses from the proximal portion of PFs after bifurcation. For the sake of simplicity, we will use the terms AA and PF synapses thereafter although the terms proximal and distal synapses (with respect to GC soma) might be more appropriate.

The EPSC amplitude of AA and PF pathways were sampled with a pair of stimulations each (Fig 1A middle panel). On average, the amplitude of the AA-EPSC during baseline recordings was 110 ±12 pA and PF-EPSC 480 ±100 pA (n = 25), and the paired pulse ratio (PPR) was PPR_{AA} 1.93 ±0.08 and PPR_{PF} 1.89 ±0.07. Inhibitory inputs were preserved, and EPSCs were often followed by outward IPSCs. After baseline recording, a protocol aimed at inducing plasticity was applied (synchronous stimulation of both inputs by a train of 15 pulses at 100 Hz, every 3 s, 100 times, in Current clamp, see Fig. 1A bottom panel). Test of the AA and PF amplitude was then resumed. Figure 1A middle panel shows an example experiment with average traces of the AA-PSC, in blue, and the PF-PSC, in orange, 5 min before (continuous line) the plasticity induction protocol, and 25-30 min after the protocol (dotted line). Subtraction traces (25-30 min - last 5 min) are shown in grey to highlight changes. The AA-EPSC amplitude is increased while the PF-EPSC amplitude is decreased. Figure 1B top panel shows the time course of 24 such experiments for the AA pathway and 25 for the PF pathway with amplitude normalised to the last 5 minutes of control before plasticity induction. It shows that on average, following the induction protocol, we observed a long term change of opposite sign of the two inputs. The AA peak EPSC amplitude increased to 162 ±15% of baseline immediately after the induction protocol and then slowly decayed within 15 mins to stabilise at a value of 131 ± 7 % 25 to 30 minutes after induction, significantly larger than the baseline (p=7e-5 one-tailed T-test, n=24). The PF-EPSC on the other hand was almost unchanged immediately after the protocol (91 ±9%) and decreased to 65 ±5 % of baseline at 25-30 min, significantly smaller than the baseline (p=1e-7 one-tailed T-test, n=25).

Figure 1B also reveals a rundown of the EPSC amplitude during the baseline period, potentially obscuring long term changes induced by plasticity. A series of control experiments was conducted to quantify the rundown (No Stim experiments, see supplementary Figure 1). After the baseline period, recording was switched to Iclamp for 5 min, but no stimulation was delivered during that period. Continuous lines Figure 1B top panel show the average time course for 17 No Stim experiments for the AA- (blue) and PF-EPSCs (orange). On average, 25 to 30 minutes after the Iclamp period, the AA-EPSC was 80 ± 6% of baseline (n= 16, significantly smaller than baseline p = 0.0004, and significantly smaller than synchronous stimulation protocol p = 10e-7) and the PF-EPSC was 81 ± 8% of baseline (N = 17, not significantly smaller than baseline p = 0.062, and not significantly larger than synchronous stimulation protocol p = 0.106), indicating a rundown of the amplitude for both pathways during experimental time, independent of the induction protocol. The extent of AA- and PF-EPSC rundown was not significantly different (n= 16 and 17 respectively, p = 0.82). These values can be used to correct long term changes. When compensating for rundown, the plasticity protocol caused a long lasting effective increase of the AA-EPSC to 164% of baseline and a decrease of the PF-EPSC to 80% of baseline on average.

Fig 1B middle panel shows the ratio of normalised AA and PF peak amplitudes (AA/PF). This measure highlights the relative amplitude change of AA and PF inputs, or relative plasticity, and eliminates changes common to both pathways, such as the rundown of synaptic responses. On average the normalised amplitude of the AA-EPSC more than doubles compared to that of the PF-EPSC, due to both the increase of the AA peak amplitude and the concomitant decrease of the PF, and this is sustained (AA/PF = 2.5 ± 0.4 with N = 24, p=3e-4 after 25-30 mins of induction). While the peak amplitude of the first response in the pair of stimulations showed a progressive decline, the peak amplitude of the second response of both AA and PF underwent either LTP or LTD respectively, and was relatively stable thereafter. Figure 1B bottom panel shows that the paired pulse ratio of normalised amplitudes (PPR) of both pathways is transiently decreased following induction, but returns to its original value within 25-30 minutes. This suggests a transient presynaptic effect on release probability and likely explains the progressive effects on AA and PF responses.

Additionally, the level of plasticity measured in a given input pathway did not depend on the amplitude of the synaptic response of that input nor on the sum of the amplitudes of the two pathways (see Supplementary Fig. 2B), showing that even relatively small inputs can trigger plasticity. We analysed the average number of spikes and the time to the first spike during the first 5 trains of stimulation of the induction protocol. All cells except one did spike, even those with relatively weak synaptic currents for

the first evoked response. The plastic change for the AA-EPSC only slightly correlated with the number of spikes (Pr = 0.48) and the time to the first spike (Pr = 0.4), and no correlation was observed for PFs (see Supplementary Fig. 2C).

To test whether the plasticity observed is due to the co-activation of AA and PF inputs or the specific properties of the stimulated inputs, we performed a series of experiments in which only one of the pathways was stimulated during the induction protocol. Figure 1C depicts the average behaviour in 8 experiments where only the AA pathway was stimulated during induction. The average amplitude of the AA-EPSC progressively decreased to 72 % ± 7% (N = 8) of control 25-30 minutes after the protocol, similarly to the PF-EPSC (64 % ± 6% of control, N = 8), not different from No Stim experiments (p = 0.49 and p= 0.48 respectively). The normalised amplitude of the AA-EPSC was not significantly different from that of the PF-EPSC following induction (AA/PF: 1.2 ± 0.2 after 25-30 min, p =0.58, N = 8, Fig. 1C bottom panel). This shows that stimulation of the AA pathway alone is not sufficient to trigger AA-LTP. Figure 1D shows the average time course of 13 experiments where only the PF pathway was stimulated during induction. In this case, the AA pathway showed a decrease (84% ± 7 % of baseline after 25-30 min, N = 12), whereas the PF pathway developed a larger depression over time (64% ± 6 % of baseline), but not different from No Stim experiments (p = 0.63 and p = 0.25 respectively). The relative amplitude of the normalized AA-EPSC (AA/PF) increased slowly after induction and was significant after 25-30 min (AA/PF = 140%± 11 % of baseline, N = 12, p = 0.01), in line with the progressive depression of the PF pathway. In these experiments, the PPR of the AA and PF pathways were transiently modified after induction, as in control, but only for the pathway stimulated during the protocol (see Fig. 1C and 1D bottom panel).

Stimulation of either pathway independently did not induce AA-LTP, showing that co-activation of AA and PF inputs is necessary, and AA-LTP is associative. The PF-EPSC was decreased following the induction protocol but this was not significantly different from control No Stim experiments.

Timing dependence of plasticity. The relative timing of inputs relates them to a common event and might be relevant to functional association, as observed for CF-mediated LTD (Safo & Regehr, 2008). We tested whether the relative timing of stimulation of the AA and PF pathways affects plasticity. During the induction protocol, the AA input was stimulated 150 ms after or 150 ms before the PF input. Figure 2A shows that when stimulating AAs 150 ms after PFs, the amplitude of the AA- and PF-EPSCs was depressed to a similar extent (AA was 53 % ± 15 % and PF 50 % ± 20 % of baseline, n = 8, not significantly different from each other p = 0.84), transforming AA-LTP into LTD. These changes were significantly

different from experiments with synchronous stimulation (p = 8e-5 for AA and p = 0.022 for PF). The relative amplitude of the AA to PF pathway increased but not significantly (AA/PF was 224 % ± 75 % of baseline, n = 8, p = 0.2). On the other hand, when stimulating AAs 150 ms before PFs (see Fig. 2B), the amplitude of the AA-EPSC was first facilitated and declined back to baseline (AA after 25-30 min was 97% ± 26%, n = 7, significantly smaller than synchronous stimulation p = 0.011), and the amplitude of the PF-EPSC was now close to baseline (84 % ± 12 %, n= 7, not significantly larger than synchronous stimulation, p = 0.062). The relative amplitude of the AA to PF pathway was not facilitated significantly (AA/PF was 126 % ± 31 % of baseline, p = 0.35), while the PPR slightly increased (PPR_{AA} = 114 % ± 6 %, p = 0.008, and PPR_{PF} = 107 % ± 5%, N = 7 and p = 0.09 respectively).

Figure 2C shows that on average, the AA-EPSC was 131% ± 7% (N = 24) fo baseline after the induction protocol when AA and PF stimulation was synchronous; it was 53% ± 15% when AA stimulation was given 150 ms after PF stimulation (N = 8), and 97 % ± 26 % (N = 7) when the PF stimulation was started 150 ms after AA stimulation. The PF-EPSC was 65 % ± 5 % of baseline (N = 25, significantly different from AA, p = $6e^{-11}$) when stimulation was synchronous, 50% ± 20% when AA stimulation was delayed by 150 ms (N = 8), and 84 % ± 12 % when PF stimulation was delayed by 150 ms (N = 7).

These experiments show that the relative timing of the AA and PF input stimulation determines the extent of plasticity of both GC synapses, sometimes in opposite directions. The AA-EPSC was either facilitated or depressed significantly.

Plasticity induction mechanism. PF-LTD and LTP have been linked to mGluR (Daniel et al., 1992; Konnerth et al., 1992; Hémart et al., 1995) and/or NMDAR activation (Casado et al., 2002; Bidoret et al., 2009; Bouvier et al., 2016; Kono et al., 2019), and KOs of either receptor show defects in cerebellar learning (Aiba et al., 1994; Nakao et al., 2019; Kono et al., 2019; Schonewille et al., 2021). mGluRs are highly expressed by PCs and located postsynaptically at GC to PC synapses. mGluRs activation requires PF train stimulation, and it has not been observed when stimulating sparse GC synapses (Marcaggi & Attwell, 2005). NMDARs on the other hand are expressed by molecular layer interneurons (Glitsch & Marty, 1999; Duguid & Smart, 2004) and GCs (Bidoret et al., 2009; Bidoret et al., 2015), where they are located on dendrites and presynaptic varicosities. We investigated the requirement for mGluR and NMDAR activation in induction of associative plasticity of the AA and PF pathways.

In figure 3A and B, mGluRs were blocked using the competitive mGluR1 antagonist CPCCOEt (50 µM). In these conditions, the AA-EPSC increased transiently following induction, but there was a long term

decrease within 25-30 minutes (AA was 72% ± 13% of baseline, statistically smaller than control synchronous stimulation, p=0.0004, N=7 and N=24). In the presence of the antagonist, the PF-EPSC was also decreased (PF was 54% ± 8 %, N=7, not significantly smaller than control synchronous stimulation, p=0.12, N=7). The transient decrease in PPR was present for both inputs, indicating no involvement of the mgluR1.

Figure 3C shows the effect of inhibiting NMDARs with the NMDAR competitive antagonist APV (50 µM) on associative AA and PF plasticity induction. With NMDARs blocked, AA-LTP observed after synchronous stimulation was completely suppressed. The AA- and PF-EPSCs were on average 50% ± 8 % and 40% ± 9% of baseline 25 to 30 minutes after induction (n = 6, significantly smaller than control p = 2e-6, and n = 7, p = 0.027 respectively). When compared to the PF pathway, depression was not significantly different at AA synapses and there was no relative amplitude change (AA/PF = 109% ± 22%, n = 5, p = 0.34) at 30 min. APV did not affect the transient depression of the PPRs. These data show that NMDAR activation is required for the associative AA-LTP described here.

These results show the concomitant involvement of both mGluRs and NMDARs in the induction of plasticity at GC synapses.

Role of inhibition. PCs receive GABAergic inhibition from molecular layer interneurons directly recruited by GCs. $GABA_A$Rs are also present on GCs, including presynaptically on the GC axon (Stell et al., 2007). These presynaptic $GABA_A$Rs are activated by synaptic release of GABA and affect the axonal Cl^- concentration and synaptic release (Stell et al., 2007; Astorga et al., 2015; Berglund et al., 2016). Several recent studies have shown that plasticity of PF-EPSCs is affected by GABAergic inhibition. Binda et al. (2016) showed that PF-LTP in mice relies on $GABA_A$R activation to hyperpolarize PC dendrites and allow recruitment of T-type Ca^{2+} channels. Rowan et al. (2018) also showed that the recruitment of molecular layer interneuron mediated inhibition can modify CF-mediated Ca^{2+} signals and LTD induction.

The role of $GABA_A$Rs-mediated inhibition was tested during plasticity induction. To this end, a series of experiments was performed with the $GABA_A$R antagonist SR95531 (3 µM) in the bath throughout the recording, and the AA and PF pathways were stimulated simultaneously (Fig. 4). With $GABA_A$Rs blocked, the AA-EPSC was initially facilitated after induction (170% ± 30%, N=9), but that potentiation decreased with time and it was 117% ± 24% of baseline after 25-30 minutes. The outcome of induction on the AA pathway was highly variable, and in 2 out of 9 cells, the AA-EPSC was strongly depressed at 25-30 min. On average, AA-LTP was smaller than in control experiments, and given the variability observed, it was

not significantly larger than control No Stim experiments (p=0.06), nor different from control experiments (p=0.1). The decrease of the PF-EPSC on the other hand was significant at 25-30 min (56±10%, N=9, significantly smaller than No Stim p=0.04) but not significantly smaller than control values (p=0.19). The relative plasticity of AA and PF inputs was stable following induction (AA/PF = 330% ±130 % at 25-30 min after induction N=9). The PPR of both pathways was transiently decreased. $GABA_AR$ activation therefore seems to be required for efficient induction and maintenance of this type of associative plasticity.

Role of synaptic inputs distribution. We have shown that paired stimulation of AA and PF triggers AA-LTP. AAs can make several synapses per axon, and these are sparsely distributed on the vertical axis of the PC dendritic tree. On the other hand, because PFs are stimulated in the molecular layer, they are stimulated as a dense beam of fibres and therefore a dense patch of synapses. We asked whether induction of AA-LTP is due to the sparse distribution of AA synapses rather than the specific properties of AA inputs.

To test for the role of the sparse distribution of the inputs, a series of experiments was performed substituting local AA stimulation with GC layer stimulation at a distance of 100 to 180 µm from the recorded PC. In this configuration, GC layer stimulation recruits PF synapses sparsely distributed on the PC dendrites and cannot involve AA synapses. The induction protocol was then applied to the sparse PF pathway (PF-sparse), together with the dense pathway stimulated in the molecular layer (PF-dense) (see Fig. 5A). Figure 5B shows an example of experiment. Traces show the PF-sparse and -dense EPSCs before and after the induction protocol and subtractions (grey) to highlight changes. 25 to 30 minutes after induction, both the sparse and dense EPSCs are reduced. Fig. 5C shows the average time course of 10 experiments. Both the sparse and dense inputs are reduced on average to 88 % ± 13% of baseline (significantly smaller than control AA, p = 0.0024, n= 10 PF-sparse and n= 24 AA control) and 54% ± 10 % of baseline (significantly smaller than control PF, p = 0.017, n= 10 PF-dense and n = 25 PF control) after 25-30 minutes respectively. When AA stimulation was replaced by sparse PF stimulation, the amplitude of the PF-sparse input was not increased as seen for AA inputs, but depressed similarly to control No Stim experiments. There was initially no change of the ratio of normalised amplitudes of the two pathways, although with time, the dense PF input stimulated in the molecular layer was more strongly depressed than the sparse input, and the relative plasticity of PF-sparse increased (PF-sparse/PF-dense = 182 % ± 24 %).

Experiments suggest that associative LTP of the AA input is not due to the sparse distribution of stimulated AA synapses on PC dendrites, but to the stimulation of a population of synapses prone to a specific form of plasticity.

Discussion

We show for the first time that stimulating AA and PF inputs simultaneously triggers LTP of the stimulated AA inputs specifically. AA-LTP is associative as it is not observed with stimulation of either pathway alone and it is timing-dependent. AA-LTP is weakly dependent on GABAergic inhibition, but most interestingly also, on the activation of both mGluRs and NMDARs. It is linked to the identity of AA synapses rather than their sparse distribution on PC dendrites, as it is not observed for sparse PF inputs. Below we discuss these findings and potential consequences for cerebellar physiology.

Identification of AA synapses. We have shown that the difference in plasticity observed between the AA and PF inputs is not linked to the distribution of synapses on the dendritic tree but to different properties of the synapses. We have argued earlier that our approach for stimulating fibres recruits mainly PF synapses, for molecular layer stimulation, and mainly AA synapses, for local GC layer stimulation. However, we have no morphological identification to verify that these are strictly AA or PF synapses. Strictly speaking, GC layer stimulation will recruit proximal synapses, close to the soma of GCs, including some formed by the PF close to the bifurcation point of the axon, whereas molecular layer stimulation will recruit mostly synapses distal from the GC somas. Alternatively, there could be a gradient of properties from proximal to distal sites. If there is a gradient however, it is limited to short distances compared to the total fibre length, as this effect was not observed when stimulating PFs in the GC layer 100-180 µm from the recorded cell (4 to 5% of the total fibre length, Fig. 5). If the plasticity described here applies to a gradient along the GC axon rather than to AAs and PFs, this would not impact the mechanisms identified nor the consequences for cerebellar physiology.

AA plasticity. To our knowledge, only Sims and Hartell (2005, 2006) examined plasticity at AA synapses and reported the absence of both LTP and LTD associated with CF conjunctive stimulation. We have observed AA-LTP with synchronous stimulation and AA-LTD when AAs were stimulated 150 ms after PFs (Fig. 2). Also, activation of both mGluRs and NMDARs is required for AA-LTP (Fig. 3). This is interesting in view of the past involvement of these receptors independently in cerebellar PF plasticity, both linked to

PF stimulation**.** The difference with previous reports lies with the simultaneous stimulation of AA with a PF beam. Number of studies have investigated the role of presynaptic NMDARs and mGluRs in cerebellar LTD and LTP (Daniel et al., 1992; Konnerth et al., 1992; Hémart et al., 1995; Lev-Ram et al., 1997; Casado et al., 2002; Bidoret et al., 2009; Bouvier et al., 2016). NMDAR and mGluR activation could take place at AA and PF synapses independently. However, the need for coincident activation of the two synaptic inputs suggests a requirement for crosstalk between the two synaptic territories and for a signal not generated at AA synapses, at least when stimulated on their own. Crosstalk could happen either through spatial overlap or signal propagation between the inputs. Our experiments used horizontal slices, where PC dendrites dip into the slice, so we have no indication whether the two synaptic territories overlap. Given the size of the inputs (Suppl. Fig. 2) however, spatial overlap is unlikely to happen in a significant proportion of experiments. This suggests that a signal needs to propagate from PF synapses.

One possibility is that NMDARs or mGluRs are absent from AA synapses. We have no information on the specific localisation of receptors at AA vs PF synapses. mGluRs in PCs activate several downstream pathways including IP_3-mediated Ca^{2+} release (Finch & Augustine, 1998; Takechi et al., 1998). mGluR-mediated Ca^{2+} signals are not expected to propagate across the PC dendritic tree, because both Ca^{2+} and IP_3 are quickly buffered, and would be an unlikely substrate for crosstalk. mGluRs activation however, also triggers the production of endocannabinoids (EC; Maejima et al., 2001; Brown et al., 2003), which can diffuse across membranes, and CB1Rs have been involved in PF-LTD (P. K. Safo & Regehr, 2005; Carey et al., 2011). Similarly, presynaptic NMDARs have been linked to LTD through release of NO which also diffuses across membranes. The NO signal generated by PF activation might be sufficient to diffuse to the AA territory. EC and NO are both potential substrates for crosstalk between AA and PF synapses.

Another possibility is that one receptor is present but fails to activate when AAs are stimulated on their own. The mGluR slow EPSC does not activate with sparse stimulation (Marcaggi & Attwell, 2005), which was attributed to insufficient build up of glutamate to activate the receptor. Canepari and Ogden (2006), however, showed that mGluR mediated Ca^{2+} release from stores is activated at lower glutamate concentration than the slow EPSC, and might therefore take place with sparse inputs, but it requires priming by depolarisation. Fluctuations of the dendritic potential triggered by the PF-EPSC could enable mGluR mediated signals at AA synapses. There is no reason however for this mechanism to distinguish sparse AA from sparse PF inputs, unless the isolation of AA synapses in fine dendritic branches (Lu et al., 2009) makes them more prone to depolarisation.

PF synapses. In the experimental conditions used here, a decrease of the PF-EPSC was induced by the co-stimulation induction protocol. It was not significantly different from the EPSC rundown, but still amounted to a 20 % decrease of the PF-EPSC when compensating for the rundown. The decrease of the PF-EPSC we observed was unexpected because the induction protocol we used, when applied to PF only, was previously shown to induce PF-LTP (Binda et al., 2016; Jörntell & Ekerot, 2002). We do not have an explanation for this difference with the study of Binda (2016), but noticeable differences are the use of mice rather than rats, but also differences in the orientation of cut of the slices, which might have resulted in the study of different cerebellar lobules. Importantly also, we used a low internal Cl^- concentration, reproducing the concentration estimated in PCs (Chavas & Marty, 2003). It is however interesting to notice that PF plasticity appears to be under the control of the CF while AA plasticity is here under the control of PFs.

Role of inhibition. Experiments were performed with inhibition preserved and $GABA_A$Rs activation was shown to secure efficient induction of AA-LTP (see Fig. 4). Block of $GABA_A$Rs did not suppress the initial increase in amplitude, but under these conditions plasticity was not sustained, highly variable and not significant when compared to No Stim experiments. Inhibition indeed seems to interfere with plasticity induction (Binda et al., 2016; Rowan et al., 2018). At this stage, we have no detail on the mechanism of influence of GABAergic inhibition in AA-LTP induction. Binda et al. (2016) showed that hyperpolarisation by IPSCs relieves inactivation of T-type Ca^{2+} channels, themselves regulated by mGluR1, boosting Ca^{2+} signals and triggering PF-LTP. That mechanism would seem compatible with our results at AA synapses although we do not know whether it requires NMDARs activation.

Cerebellar physiology. Importantly, this work shows that the climbing fibre is not the only key to associative plasticity in PCs. Despite the large dimensions of the PC dendritic tree and the small inputs involved, it shows that integration at the level of the PC dendrites only requires moderate inputs to spread and trigger plasticity. It is a surprise, given that associative plasticity of GC inputs has only been described in association with the powerful CF input, which triggers widespread depolarisation and Ca^{2+} increase.

Anatomical data suggest that a large proportion of AA synapses are targeted to specific fine branches of the PC dendrites and segregated away from CF and PF synapses (Lu et al., 2009). These and the present study suggest that AA synapses are a different population of GC synapses. The anatomical differences between AAs and PFs might be coupled to molecular and functional differences, taking advantage of the

geometric organisation of the cerebellar cortex to encode information. Plasticity of AA synapses will need to be further examined with respect to the CF and local inhibition to check whether the CF specifically controls PF plasticity.

We argued in the introduction that, as a consequence of morphology, AAs can only form synapses with a few PCs, while PFs course through and synapse with the dendrites of hundreds of PCs. AA synapses are suited to encode precise and selective information from the receptive field, while PF synapses could efficiently represent context. This work comforts the idea that they are functionally different and might fulfil distinct roles with respect to the computation performed by the cerebellar cortex. The associative form of plasticity we describe is expected to increase the contrast between AA and PF inputs in a time dependent manner, reinforcing AA signals presented conjointly with PF, while attenuating signals presented in isolation. The time dependence of plasticity is of particular interest as it allows for modification of the inputs in relation to the timing of presentation, as expected for motor and sensory feedback information, which require pertinent association. It will be interesting to study inhibitory signals further in this context to see whether they participate in creating a negative image of the excitatory signals, as observed in cerebellar-like structures.

Acknowledgements. We would like to dedicate this work to the memory of David Ogden, who was influential in placing the cerebellum at the center of this work. We thank Brandon Stell and Alain Marty for discussions on the manuscript. We thank the Animal Housing and Breeding facility and the Prototyping facility of BioMedTech facilities (INSERM US36, CNRS UAR2009, Université Paris Cité) for providing the animals used in this study and assistance with technical developments. The work was funded by ANR grants ANR-19-CE37-011-01 SpinoCereLoco and ANR-18-CE16-0010-01 RewardInhib.

Figure legend:

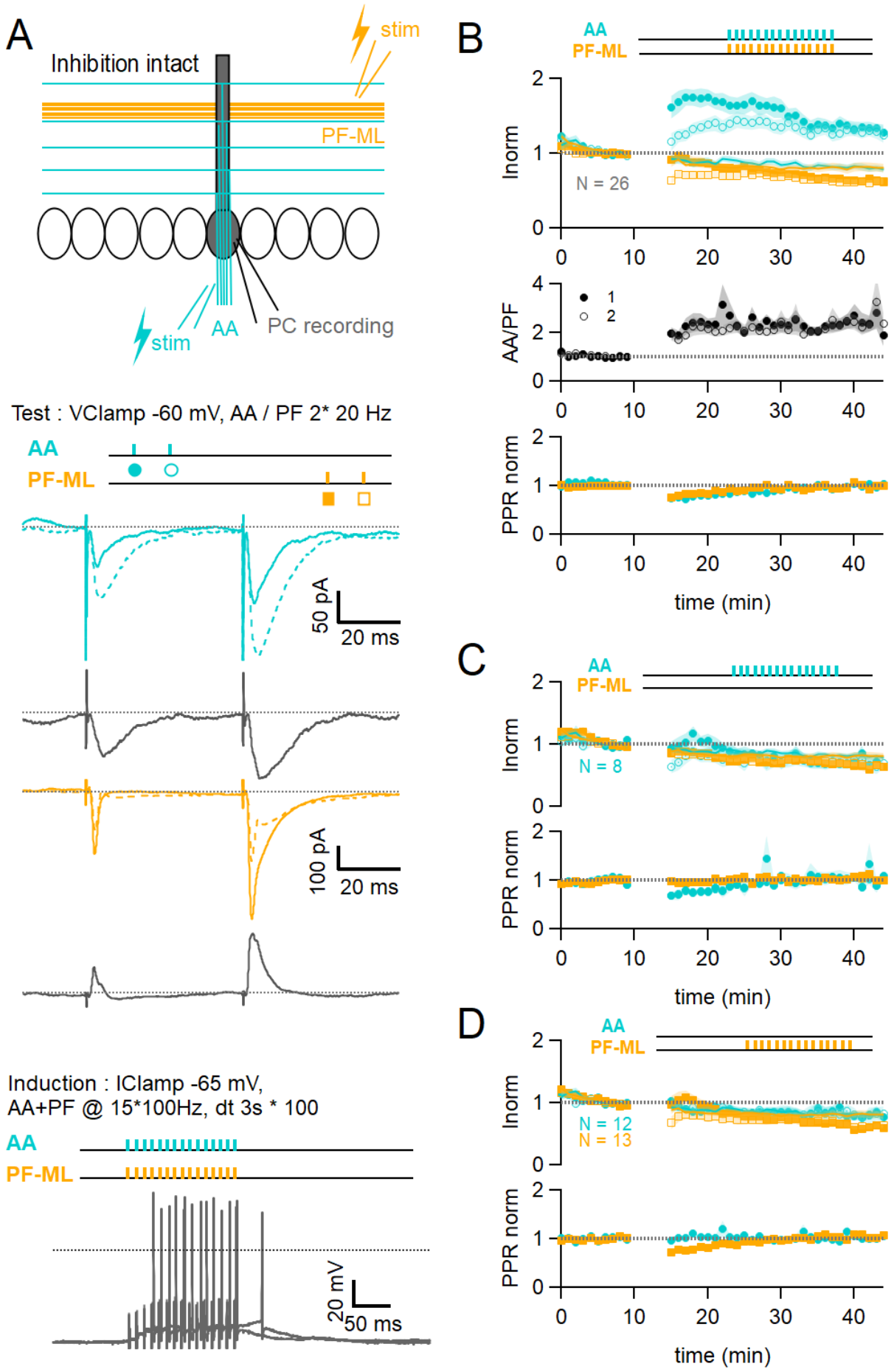
A
Inhibition intact
stim
PF-ML
stim
AA
PC recording
Test : VClamp -60 mV, AA / PF 2* 20 Hz
AA
PF-ML
50 pA
20 ms
100 pA
20 ms
Induction : IClamp -65 mV,
AA+PF @ 15*100Hz, dt 3s * 100
AA
PF-ML
20 mV
50 ms
B
AA
PF-ML
Inorm
N = 26
AA/PF
1
2
PPR norm
time (min)
C
AA
PF-ML
Inorm
N = 8
PPR norm
time (min)
D
AA
PF-ML
Inorm
N = 12
N = 13
PPR norm
time (min)

Figure 1: Associative plasticity of AA and PF inputs. A, top. Whole cell recording in a PC. Two stimulation electrodes are used to activate GC inputs: one in the molecular layer to stimulate PFs (orange), and one in the GC layer to stimulate AAs (blue). **Middle**, AA- and PF-PSCs sampled with a pair of pulses (dt = 50 ms), every 10 s. Traces from one experiment: average AA-PSC (blue) and PF-PSC (orange), before (5-10 min, continuous line) and after the induction protocol (25-30 min, dotted line). Subtraction in grey. AA-EPSC amplitude increased while PF-EPSC amplitude decreased. No antagonist was applied. Evoked responses often consisted of mixed EPSC/IPSC. **Bottom**, induction protocol. Recording switched to current clamp, V_H = -65 mV. AAs and PFs are stimulated synchronously by a train of 15 pulses at 100 Hz every 3 s for 5 min. Grey traces, responses to the first two trains of stimulation. **B Top**, plot of the average AA- and PF-EPSC amplitude normalised to baseline (5-10min, n = 25, colours and symbols as in A) for LTP and control No Stim experiments (continuous lines). Following induction, a long term change of opposite sign of the inputs was observed. The amplitude of the AA-EPSC increased to 131% ± 7 % (N = 24) of baseline 25-30 min after induction. The PF-EPSC on the other hand decreased slowly to 65% ±5 % (N = 25) of baseline. Continuous lines show the average time course of AA- and PF-EPSC amplitudes during control No Stim experiments where no stimulation was performed during the Iclamp period (N = 17, see supplementary Figure 1), showing the extent of EPSC rundown during the course of the recordings. **Middle**, the average ratio of the normalised amplitudes of AA- and PF-EPSCs (AA/PF), highlighting the relative change of the inputs (relative plasticity), doubles. **Bottom**, average normalised paired pulse ratio (AA2/AA1 and PF2/PF1) is transiently decreased following induction. **C.** Average of 8 experiments with stimulation of the AA pathway only during induction (labels, colours and symbols as in A), and No Stim experiments overlaid (continuous lines). **Top**, the normalised amplitudes of AA- and PF-EPSCs progressively decreased to 72 % ± 7% (N = 8) and 64 % ± 6% (N = 8) of baseline respectively at 25-30 minutes, not significantly different from No Stim experiments. Stimulation of the AA pathway alone is not sufficient to trigger AA-LTP. **D.** Average of 13 experiments with stimulation of the PF pathway only during induction (labels), and No Stim experiments overlaid (continuous lines). **Top**, the normalised AA-EPSCs showed a small and steady depression (84% ± 7 % of baseline after 25-30 min) whereas the PF-EPSC depressed over time (64% ± 6 %), not significantly different from No Stim experiments. Stimulation of the PF pathway on its own is not sufficient to trigger LTP or LTD. **C** and **D bottom**, the PPR of the AA and PF pathways transiently decreased only for the pathway stimulated during induction.

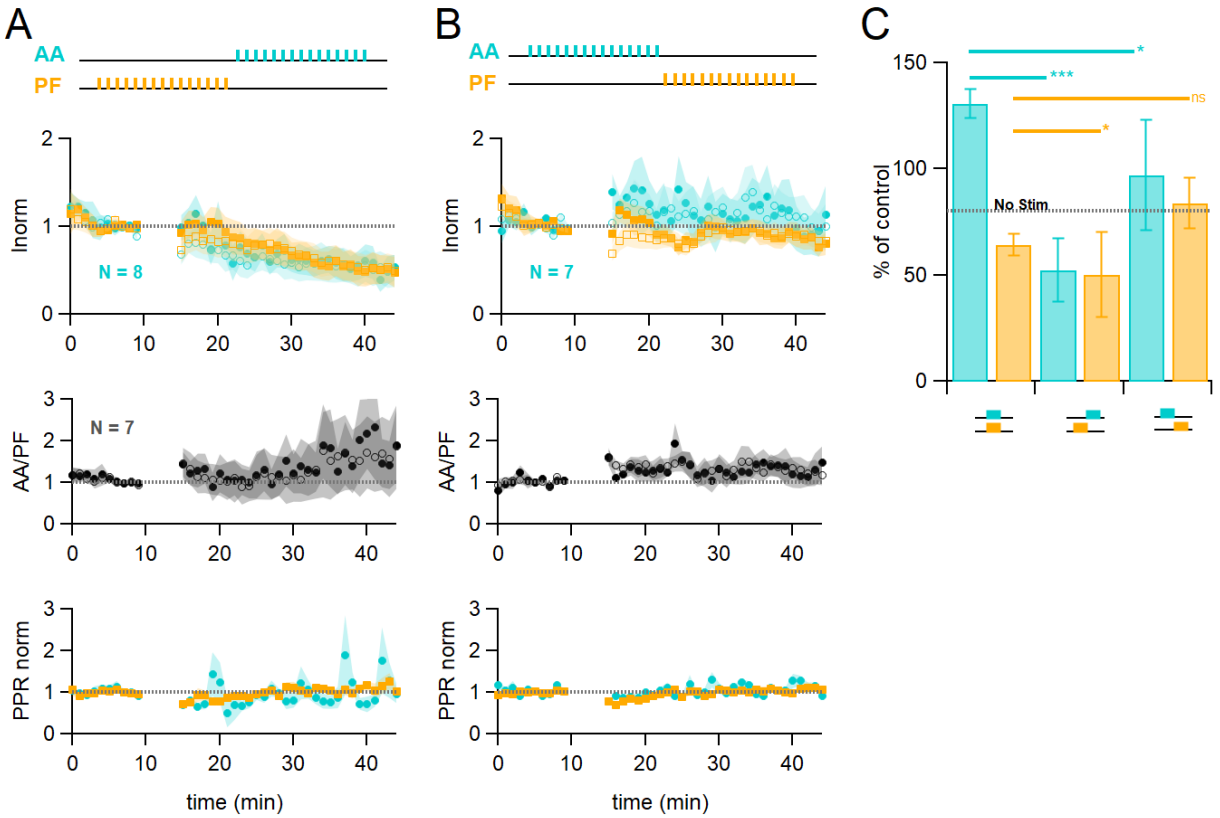

Figure 2: Time dependence of plasticity. The effect of the relative timing of stimulation of the AA and PF pathways on plasticity was tested by stimulating the AA input 150 ms after or 150 ms before the PF input. **A.** On average, when stimulating AAs 150 ms after PFs, the AA- and PF-EPSCs now decreased by a similar extent (AA was 53 % ± 15 %, PF 50 % ± 20 % of control, n = 8). The relative normalised amplitude of the AA pathway increased but not significantly (AA/PF was 224 % ± 75 % of control, n = 7). **B.** When stimulating AAs 150 ms before PFs, the AA-EPSC first facilitated, but declined back to baseline (AA was 97% ± 26% of control, n = 7), and the PF-EPSC was maintained close to baseline (PF 84 % ± 12 % of control, n= 7). The relative normalised amplitude of the AA pathway and the PPR were not affected significantly (AA/PF was 126 % ± 31% of control, and PPR_{AA} = 114.4 % ± 6.4 %, PPR_{PF} = 107.1 % ± 4.6%, N = 7). **C.** Average amplitude as a percentage of baseline at 25-30 min. The dotted line shows the value of EPSC amplitude at the end of No Stim experiments. The AA-EPSC was 131% ± 7% of baseline (N = 24) 25 to 30 min after induction when AA and PF stimulation was synchronous. It was 53% ± 15% (N = 8) when AA stimulation was delayed by 150 ms, and 97 % ± 26 % (N = 7) when PF stimulation was delayed by 150 ms. The PF-EPSC was 65 % ± 5 % of baseline (N = 25) when stimulation was synchronous, 50% ± 20% (N = 8) when AA stimulation was delayed by 150 ms, and 84 % ± 12 % (N = 7) when PF stimulation was delayed by 150 ms. (*** $p \leqslant 0.001$, * $p \leqslant 0.05$, ns: not significant).

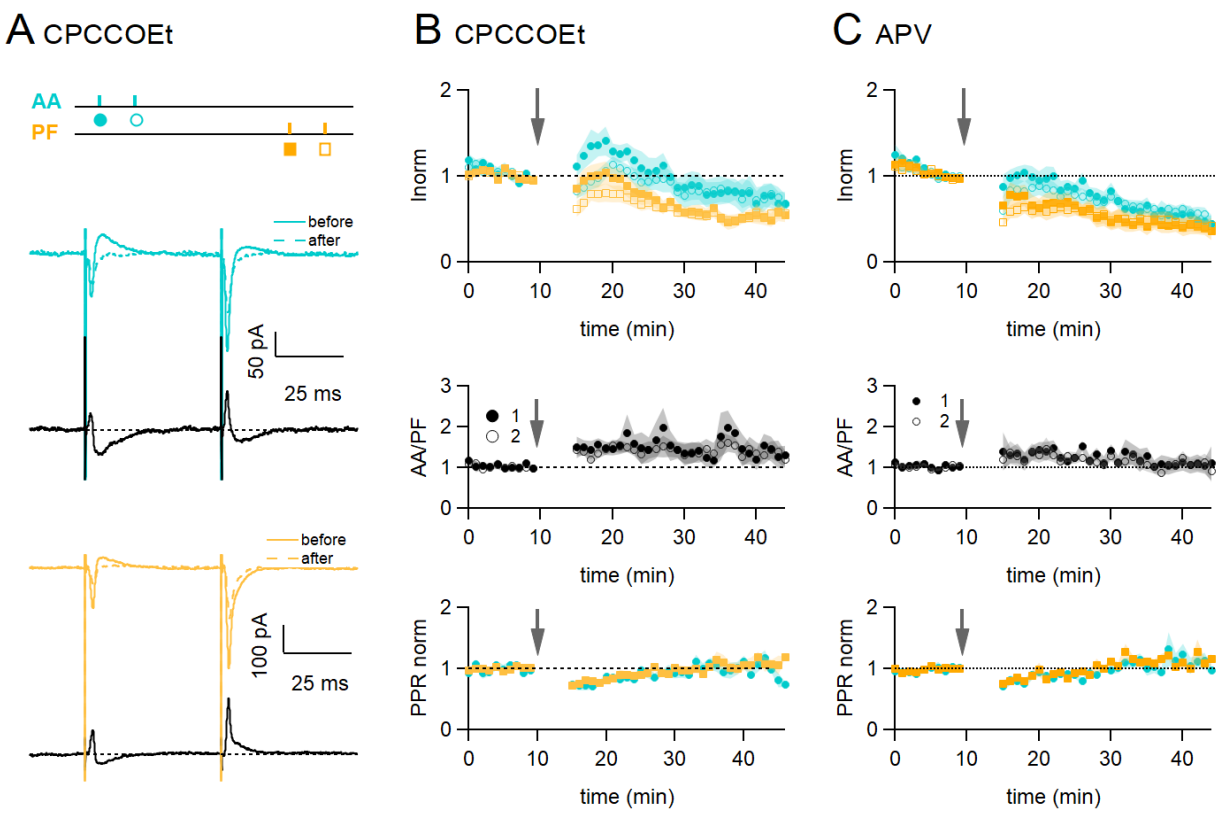

Figure 3: Role of NMDARs and mGluRs. A. Bath application of CPCCOEt (50 µM), a selective blocker of mGluR1Rs, strongly inhibits LTP of AA-EPSCs. Sample recordings from one experiment. Traces are the average of the AA(blue) and PF (orange) synaptic responses, before (5-10 min, continuous line) and after induction (25-30 min, dotted line). Subtraction traces (25-30 min - 5-10min) in black. A decrease of the AA-EPSC is observed, and the PF-EPSC is decreased as in control experiments. **B. Top**: Average time course of the normalised AA- and PF-EPSCs (N = 8). mGluR1 receptor block impairs AA-LTP. **Middle**: a small sustained increase of the ratio of normalised amplitudes (AA/PF) is observed. **Bottom**: Plot of the normalised PPR of both inputs. mGluR1R block does not influence the transient decrease in PPR following induction. **C.** Average of 7 experiments in the presence of the NMDAR competitive antagonist APV (50 µM). **Top**: Average normalised AA- and PF-EPSC amplitudes as a function of time (colours and symbols as in A). Following induction in the presence of APV, both AA and PF pathways are depressed, showing that NMDAR activation is necessary for AA-LTP induction. **Middle**: The ratio of normalised amplitudes (AA/PF) is slightly increased, reflecting a slower depression of the AA inputs. **Bottom**: the transient decrease of the normalised PPRs is still observed.

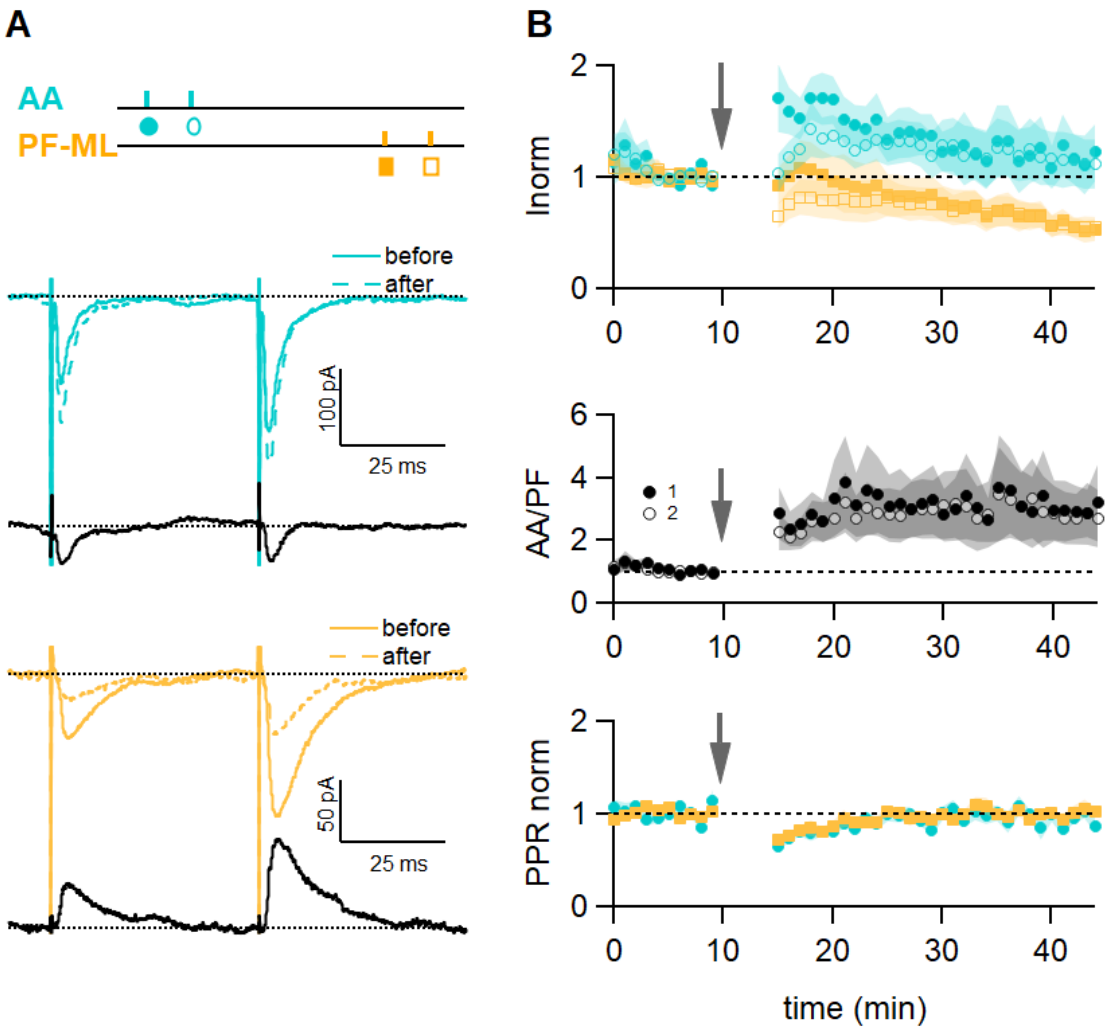

Figure 4: $GABA_A$ receptor block affects long term plastic changes. A. Sample recordings from an experiment in the presence of the $GABA_AR$ antagonist SR (3 µM). Paired EPSCs evoked before and after induction, together with subtraction traces (black), are shown for the AA (blue) and PF (orange) pathways. The AA-EPSC is increased after induction and the PF-EPSC is strongly decreased in this experiment. **B.** Average normalised peak EPSC amplitudes of the first and second evoked responses for AA and PF for 9 experiments. The big errors in AA peak amplitude observed after induction are due to the large variability of the outcome of the protocol on this pathway (AA 117%± 24 % ; PF 56%± 10%, n = 9). The ratio of the normalised AA and PF amplitude shows the same variability, while the normalised PPR displays the same relative error and time course as control experiments.

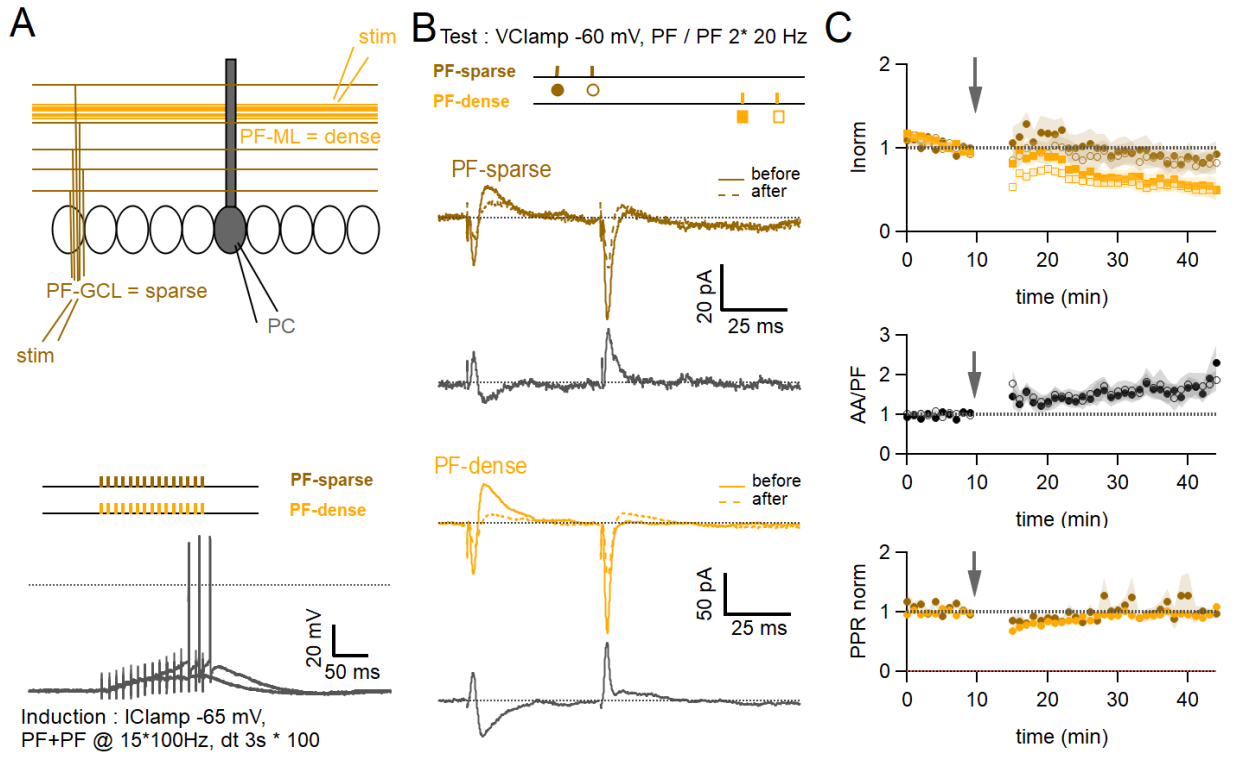

Figure 5: Role of the sparse input distribution. A. To test the role of the sparse input distribution, a stimulation electrode was positioned in the GC layer, 100 to 180 µm from the recorded PC, stimulating only PF synapses sparsely distributed on the PC dendrites. The induction protocol was applied to the sparse PF pathway (PF-sparse), together with the dense PF pathway stimulated in the molecular layer (PF-dense). **B.** Example experiment. Traces show the PF-sparse and -dense EPSCs before and after induction, and subtractions (grey) to highlight changes. 25 to 30 minutes after induction, both the sparse and dense EPSCs are reduced. **Bottom left**, IClamp responses to the first two trains of stimulation. **C.** Average time course of the normalised EPSC amplitudes for 10 experiments. Both sparse and dense inputs (colours and symbols as in B, top) are reduced on average to 88 % ± 13% (significantly smaller than control AA, p = 0.0024, n= 10 PF-sparse and n= 24 AA control) and 54% ± 10 % of baseline (significantly smaller than control PF, p = 0.017, n= 10 PF-dense and n = 25 PF control) after 25-30 min respectively. When AA stimulation was replaced by sparse PF stimulation, the PF-sparse input was depressed over the following 30 minutes, similarly to the PF-dense input. With time, the dense PF input was more strongly depressed, and the ratio of normalised amplitudes (PF-sparse/PF-dense) increased to 182 % ± 24 % of control.

References

Aiba, A., Kano, M., Chen, C., Stanton, M. E., Fox, G. D., Herrup, K., Zwingman, T. A., & Tonegawa, S. (1994). Deficient cerebellar long-term depression and impaired motor learning in mGluR1 mutant mice. *Cell*, *79*(2), 377–388.

Astorga, G., Bao, J., Marty, A., Augustine, G. J., Franconville, R., Jalil, A., Bradley, J., & Llano, I. (2015). An excitatory GABA loop operating in vivo. *Frontiers in Cellular Neuroscience*, *9*, 275. https://doi.org/10.3389/fncel.2015.00275

Berglund, K., Wen, L., Dunbar, R. L., Feng, G., & Augustine, G. J. (2016). Optogenetic Visualization of Presynaptic Tonic Inhibition of Cerebellar Parallel Fibers. *The Journal of Neuroscience: The Official Journal of the Society for Neuroscience*, *36*(21), 5709–5723. https://doi.org/10.1523/JNEUROSCI.4366-15.2016

Bidoret, C., Ayon, A., Barbour, B., & Casado, M. (2009). Presynaptic NR2A-containing NMDA receptors implement a high-pass filter synaptic plasticity rule. *Proceedings of the National Academy of Sciences of the United States of America*, *106*(33), 14126–14131. https://doi.org/10.1073/pnas.0904284106

Bidoret, C., Bouvier, G., Ayon, A., Szapiro, G., & Casado, M. (2015). Properties and molecular identity of NMDA receptors at synaptic and non-synaptic inputs in cerebellar molecular layer interneurons. *Frontiers in Synaptic Neuroscience*, *7*, 1. https://doi.org/10.3389/fnsyn.2015.00001

Binda, F., Dorgans, K., Reibel, S., Sakimura, K., Kano, M., Poulain, B., & Isope, P. (2016). Inhibition promotes long-term potentiation at cerebellar excitatory synapses. *Scientific Reports*, *6*, 33561. https://doi.org/10.1038/srep33561

Brown, S. P., Brenowitz, S. D., & Regehr, W. G. (2003). Brief presynaptic bursts evoke synapse-specific retrograde inhibition mediated by endogenous cannabinoids. *Nature Neuroscience*, *6*(10), 1048–1057. https://doi.org/10.1038/nn1126

Bouvier, G., Higgins, D., Spolidoro, M., Carrel, D., Mathieu, B., Léna, C., Dieudonné, S., Barbour, B., Brunel, N., & Casado, M. (2016). Burst-Dependent Bidirectional Plasticity in the Cerebellum Is Driven by Presynaptic NMDA Receptors. *Cell Reports*, *15*(1), 104–116. https://doi.org/10.1016/j.celrep.2016.03.004

Canepari, M., & Ogden, D. (2006). Kinetic, pharmacological and activity-dependent separation of two Ca2+ signalling pathways mediated by type 1 metabotropic glutamate receptors in rat Purkinje neurones. *The Journal of Physiology*, *573*(Pt 1), 65–82. https://doi.org/10.1113/jphysiol.2005.103770

Carey, M. R., Myoga, M. H., McDaniels, K. R., Marsicano, G., Lutz, B., Mackie, K., & Regehr, W. G. (2011). Presynaptic CB1 receptors regulate synaptic plasticity at cerebellar parallel fiber synapses. *Journal of Neurophysiology*, *105*(2), 958–963. https://doi.org/10.1152/jn.00980.2010

Casado, M., Isope, P., & Ascher, P. (2002). Involvement of presynaptic N-methyl-D-aspartate receptors in cerebellar long-term depression. *Neuron*, *33*(1), 123–130. https://doi.org/10.1016/s0896-6273(01)00568-2

Chavas, J., & Marty, A. (2003). Coexistence of excitatory and inhibitory GABA synapses in the cerebellar interneuron network. *The Journal of Neuroscience: The Official Journal of the Society for Neuroscience*, *23*(6), 2019–2031.

Coesmans, M., Weber, J. T., De Zeeuw, C. I., & Hansel, C. (2004). Bidirectional parallel fiber plasticity in the cerebellum under climbing fiber control. *Neuron*, *44*(4), 691–700. https://doi.org/10.1016/j.neuron.2004.10.031

Cohen, D., & Yarom, Y. (1998). Patches of synchronized activity in the cerebellar cortex evoked by mossy-fiber stimulation: Questioning the role of parallel fibers. *Proceedings of the National Academy of Sciences of the United States of America*, *95*(25), 15032–15036. https://doi.org/10.1073/pnas.95.25.15032

Daniel, H., Hemart, N., Jaillard, D., & Crepel, F. (1992). Coactivation of metabotropic glutamate receptors and of voltage-gated calcium channels induces long-term depression in cerebellar Purkinje cells in vitro. *Experimental Brain Research*, *90*(2), 327–331. https://doi.org/10.1007/BF00227245

Devi, S. P. S., Howe, J. R., & Auger, C. (2016). Train stimulation of parallel fibre to Purkinje cell inputs reveals two populations of synaptic responses with different receptor signatures. *The Journal of Physiology*, *594*(13), 3705–3727. https://doi.org/10.1113/JP272415

Duguid, I. C., & Smart, T. G. (2004). Retrograde activation of presynaptic NMDA receptors enhances GABA release at cerebellar interneuron-Purkinje cell synapses. *Nature Neuroscience*, *7*(5), 525–533. https://doi.org/10.1038/nn1227

Ekerot, C. F., & Jörntell, H. (2001). Parallel fibre receptive fields of Purkinje cells and interneurons are climbing fibre-specific. *The European Journal of Neuroscience*, *13*(7), 1303–1310. https://doi.org/10.1046/j.0953-816x.2001.01499.x

Finch, E. A., & Augustine, G. J. (1998). Local calcium signalling by inositol-1,4,5-trisphosphate in Purkinje cell dendrites. *Nature*, *396*(6713), 753–756. https://doi.org/10.1038/25541

Glitsch, M., & Marty, A. (1999). Presynaptic effects of NMDA in cerebellar Purkinje cells and interneurons. *The Journal of Neuroscience: The Official Journal of the Society for Neuroscience*, *19*(2), 511–519. https://doi.org/10.1523/JNEUROSCI.19-02-00511.1999

Hémart, N., Daniel, H., Jaillard, D., & Crépel, F. (1995). Receptors and second messengers involved in long-term depression in rat cerebellar slices in vitro: A reappraisal. *The European Journal of Neuroscience*, *7*(1), 45–53. https://doi.org/10.1111/j.1460-9568.1995.tb01019.x

Ichikawa, R., Hashimoto, K., Miyazaki, T., Uchigashima, M., Yamasaki, M., Aiba, A., Kano, M., & Watanabe, M. (2016). Territories of heterologous inputs onto Purkinje cell dendrites are segregated by mGluR1-dependent parallel fiber synapse elimination. *Proceedings of the National Academy of Sciences of the United States of America*, *113*(8), 2282–2287.

https://doi.org/10.1073/pnas.1511513113

Isope, P., & Barbour, B. (2002). Properties of unitary granule cell—>Purkinje cell synapses in adult rat cerebellar slices. *The Journal of Neuroscience: The Official Journal of the Society for Neuroscience*, *22*(22), 9668–9678. https://doi.org/10.1523/JNEUROSCI.22-22-09668.2002

Jörntell, H., & Ekerot, C.-F. (2002). Reciprocal bidirectional plasticity of parallel fiber receptive fields in cerebellar Purkinje cells and their afferent interneurons. *Neuron*, *34*(5), 797–806. https://doi.org/10.1016/s0896-6273(02)00713-4

Konnerth, A., Dreessen, J., & Augustine, G. J. (1992). Brief dendritic calcium signals initiate long-lasting synaptic depression in cerebellar Purkinje cells. *Proceedings of the National Academy of Sciences of the United States of America*, *89*(15), 7051–7055. https://doi.org/10.1073/pnas.89.15.7051

Kono, M., Kakegawa, W., Yoshida, K., & Yuzaki, M. (2019). Interneuronal NMDA receptors regulate long-term depression and motor learning in the cerebellum. *The Journal of Physiology*, *597*(3), 903–920. https://doi.org/10.1113/JP276794

Lev-Ram, V., Jiang, T., Wood, J., Lawrence, D. S., & Tsien, R. Y. (1997). Synergies and coincidence requirements between NO, cGMP, and Ca2+ in the induction of cerebellar long-term depression. *Neuron*, *18*(6), 1025–1038. https://doi.org/10.1016/s0896-6273(00)80340-2

Lu, H., Esquivel, A. V., & Bower, J. M. (2009). 3D electron microscopic reconstruction of segments of rat cerebellar Purkinje cell dendrites receiving ascending and parallel fiber granule cell synaptic inputs. *The Journal of Comparative Neurology*, *514*(6), 583–594. https://doi.org/10.1002/cne.22041

Maejima, T., Hashimoto, K., Yoshida, T., Aiba, A., & Kano, M. (2001). Presynaptic inhibition caused by retrograde signal from metabotropic glutamate to cannabinoid receptors. *Neuron*, *31*(3), 463–475. https://doi.org/10.1016/s0896-6273(01)00375-0

Marcaggi, P., & Attwell, D. (2005). Endocannabinoid signaling depends on the spatial pattern of synapse activation. *Nature Neuroscience*, *8*(6), 776–781. https://doi.org/10.1038/nn1458

Montgomery, J. C., & Bodznick, D. (1994). An adaptive filter that cancels self-induced noise in the electrosensory and lateral line mechanosensory systems of fish. *Neuroscience Letters*, *174*(2), 145–148. https://doi.org/10.1016/0304-3940(94)90007-8

Nakao, H., Kishimoto, Y., Hashimoto, K., Kitamura, K., Yamasaki, M., Nakao, K., Watanabe, M., Kano, M., Kirino, Y., & Aiba, A. (2019). MGluR1 in cerebellar Purkinje cells is essential for the formation but not expression of associative eyeblink memory. *Scientific Reports*, *9*(1), 7353. https://doi.org/10.1038/s41598-019-43744-z

Napper, R. M., & Harvey, R. J. (1988). Number of parallel fiber synapses on an individual Purkinje cell in the cerebellum of the rat. *The Journal of Comparative Neurology*, *274*(2), 168–177. https://doi.org/10.1002/cne.902740204

Pichitpornchai, C., Rawson, J. A., & Rees, S. (1994). Morphology of parallel fibres in the

cerebellar cortex of the rat: An experimental light and electron microscopic study with biocytin. *The Journal of Comparative Neurology*, *342*(2), 206–220. https://doi.org/10.1002/cne.903420205

Rowan, M. J. M., Bonnan, A., Zhang, K., Amat, S. B., Kikuchi, C., Taniguchi, H., Augustine, G. J., & Christie, J. M. (2018). Graded Control of Climbing-Fiber-Mediated Plasticity and Learning by Inhibition in the Cerebellum. *Neuron*, *99*(5), 999-1015.e6. https://doi.org/10.1016/j.neuron.2018.07.024

Safo, P. K., & Regehr, W. G. (2005). Endocannabinoids control the induction of cerebellar LTD. *Neuron*, *48*(4), 647–659. https://doi.org/10.1016/j.neuron.2005.09.020

Safo, P., & Regehr, W. G. (2008). Timing dependence of the induction of cerebellar LTD. *Neuropharmacology*, *54*(1), 213–218. https://doi.org/10.1016/j.neuropharm.2007.05.029

Sawtell, N. B. (2017). Neural Mechanisms for Predicting the Sensory Consequences of Behavior: Insights from Electrosensory Systems. *Annual Review of Physiology*, *79*, 381–399. https://doi.org/10.1146/annurev-physiol-021115-105003

Schmahmann, J. D., & Sherman, J. C. (1998). The cerebellar cognitive affective syndrome. *Brain: A Journal of Neurology*, *121 (Pt 4)*, 561–579. https://doi.org/10.1093/brain/121.4.561

Schonewille, M., Girasole, A. E., Rostaing, P., Mailhes-Hamon, C., Ayon, A., Nelson, A. B., Triller, A., Casado, M., De Zeeuw, C. I., & Bouvier, G. (2021). NMDARs in granule cells contribute to parallel fiber-Purkinje cell synaptic plasticity and motor learning. *Proceedings of the National Academy of Sciences of the United States of America*, *118*(37), e2102635118. https://doi.org/10.1073/pnas.2102635118

Sims, R. E., & Hartell, N. A. (2005). Differences in transmission properties and susceptibility to long-term depression reveal functional specialization of ascending axon and parallel fiber synapses to Purkinje cells. *The Journal of Neuroscience: The Official Journal of the Society for Neuroscience*, *25*(12), 3246–3257. https://doi.org/10.1523/JNEUROSCI.0073-05.2005

Sims, R. E., & Hartell, N. A. (2006). Differential susceptibility to synaptic plasticity reveals a functional specialization of ascending axon and parallel fiber synapses to cerebellar Purkinje cells. *The Journal of Neuroscience: The Official Journal of the Society for Neuroscience*, *26*(19), 5153–5159. https://doi.org/10.1523/JNEUROSCI.4121-05.2006

Stell, B. M., Rostaing, P., Triller, A., & Marty, A. (2007). Activation of presynaptic GABA(A) receptors induces glutamate release from parallel fiber synapses. *The Journal of Neuroscience: The Official Journal of the Society for Neuroscience*, *27*(34), 9022–9031. https://doi.org/10.1523/JNEUROSCI.1954-07.2007

Stoodley, C. J., & Schmahmann, J. D. (2010). Evidence for topographic organization in the cerebellum of motor control versus cognitive and affective processing. *Cortex; a Journal Devoted to the Study of the Nervous System and Behavior*, *46*(7), 831–844. https://doi.org/10.1016/j.cortex.2009.11.008

Walter, J. T., Dizon, M.-J., & Khodakhah, K. (2009). The functional equivalence of ascending and

parallel fiber inputs in cerebellar computation. *The Journal of Neuroscience: The Official Journal of the Society for Neuroscience*, *29*(26), 8462–8473. https://doi.org/10.1523/JNEUROSCI.5718-08.2009

Takechi, H., Eilers, J., & Konnerth, A. (1998). A new class of synaptic response involving calcium release in dendritic spines. *Nature*, *396*(6713), 757–760. https://doi.org/10.1038/25547